Circular polarized incident light scattering properties at optical clearing in tissues

Dongsheng Chen,[a,b] Nan Zeng,[a] Yunfei Wang,[a,b] Honghui He,[a] Valery V.Tuchin,[c,d,e] Hui Ma,[a,b*]

[a]Shenzhen Key Laboratory for Minimal Invasive Medical Technologies, Institute of Optical Imaging and Sensing, Graduate School at Shenzhen, Tsinghua University, Shenzhen 518055, China

[b]Department of Physics, Tsinghua University, Beijing 100084, China

[c] Saratov National Research State University, 83 Astrakhanskaya Street, Saratov 410012, Russia

[d] Tomsk National Research State University, 36 Lenin Avenue, Tomsk 634050, Russia

[e]Institute of Precision Mechanics and Control of RAS, 24 Rabochaya Street, Saratov 410028, Russia

[*]Address all correspondence to: Hui Ma, E-mail: mahui@tsinghua.edu.cn

Abstract: This paper focuses on polarization imaging during optical clearing process in tissues due to refractive index matching of tissue structural components. We start with some single-dispersed tissue models, composed of large spheres, small spheres, and large cylinders, respectively. Along with the simulated refractive index matching inside and outside the scatterers, the linear polarized incident photons show similar decreased depolarization. It is worth noting that the circular polarized incident light show different polarization change for different scatterers, sensitive to scatterer size and shape. For small Rayleigh-like spherical scatterers, the circular depolarization also decreases with index matching. However, the depolarization by the larger scatterers can be enhanced, supported by the photon distribution change with the index matching in the backward detection. After some extreme points, the depolarization of circular polarized photons will be suppressed until almost disappear. Furthermore, by the simulation of hybrid-dispersed models, we can find out that the transmission of circular polarized photons during optical clearing, is more sensitive to the content of smaller scatterers in the turbid medium, and also has a close relationship with the proportion of the anisotropic scatterers. We also extract a character to describe the difference of linear and circular polarized photons. The value and the change of this character can help us to explain the main scatterers contributed to the polarization features of tissue-like medium during optical clearing. The above results indicate different polarization features for different scattering systems by optical clearing, which are potentially useful for studying optical clearing by polarization methods.

Key Words: circular polarization, scattering, optical clearing

1. Introduction

Polarimetry has been widely applied in biomedicine area [1-2]. Through polarization measurements, a lot of information such as the microstructures and optical anisotropy of the tissue can be acquired. As many physiological abnormalities change structures of tissues and cells, polarimetry has been used to detect and differentiate pathological tissues widely [3-5]. Circular polarization has the

Optical Modeling and Performance Predictions VIII, edited by Mark A. Kahan, Marie B. Levine-West, Proc. of SPIE Vol. 9953, 995308 · © 2016 SPIE
CCC code: 0277-786X/16/$18 · doi: 10.1117/12.2238789

polarization memory effect and transports a relatively longer distance in Mie scattering media, which recently has been studied much [6-7]. However, since most biological tissues are optically turbid, photons experience multiple scattering and lose polarization during the transmission in the tissues which limits the imaging depths of polarization measurements. It is urgent to increase the imaging depth and contrast of polarization imaging. One kind of the prevalent methods to fulfill it is the tissue optical clearing method, which can be used to reduce the scattering to make the tissue more transparent and has been applied successfully in optical coherence tomography, laser speckle imaging, fluorescence imaging and so on [8-12]. To be noted, recently tissue clearing techniques have been developed fast in biomedicine, for example, through the combination of advanced microscopy, labeling and optical clearing techniques, 3-D whole brain of raft has been imaging successfully with unprecedented resolution [9, 11].

However, at present the study of optical clearing technique applied in polarization measurements is not much [13-15]. Since the scattering originates from the discrepancy of the refractive index of scatterers and the interstitial medium, the most important mechanism of optical clearing techniques is the refractive index matching [10], especially for the simple cases using aqueous suspension phantoms as the samples, since the diffuse process of optical clearing agent is negligible [16]. As a preliminary attempt, in the context, we focus on the study of the influence of the refractive index matching on the polarization properties of varied simplified tissue models including those consisted of pure components such as Rayleigh-like spherical particles, Mie-like spherical particles, infinite-long cylindrical particles, and hybrid components. The linearly and circularly polarizing properties and their differences during the index matching process are examined, and as will be shown later, the circular depolarization as well as the differences of linear and circular polarization properties during the process contains more information and can reflect the unique properties of scattering systems.

The remaining parts are arranged as follows. Part 2 is the theory and method which contain Monte Carlo models and simulations, and polarization metrics. Part 3 is the results and discussions. The last part is the conclusion.

2. Theory and Method

In order to analyze the optical clearing mechanism and the polarization phenomenon during the optical clearing process systematically, we first conduct Monte Carlo simulations on the polarization features during the refractive index matching process. Based on our sphere-cylinder-birefringence model and simulation program [17-18], whose sketch map is shown in Fig.1, we study pure isotropic systems of spherical particles of Rayleigh-like or Mie-scattering, pure anisotropic systems of infinite-long cylindrical particles of large size, and hybrid systems containing two different scattering particles. The initial reduced scattering coefficients for the

systems are ranged from 1/cm to 10/cm. The thicknesses of the samples are 1cm, which are on the same scale with the corresponding depolarization lengths [19]. To be noted, for infinite-long cylindrical scattering systems, there is no definition for reduced scattering coefficient and the scattering coefficient used is similar with that of spherical scattering systems of scatterers of the same size. The Mueller matrix is derived by sum of the Mueller matrix of backward detected area of 1cm*1cm.

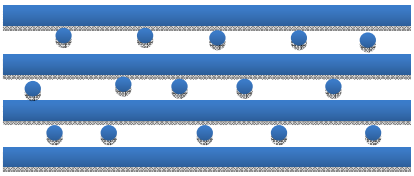

Fig. 1 The sketch map of sphere-cylinder-birefringence model

The polarization analysis methods used include Mueller matrix Polar Decomposition (MMPD) methods and some parameters originated from the matrix elements [20, 21]. The MMPD method divides an arbitrary Mueller matrix into three sub-matrix, including the depolarization matrix M_Δ, the retardance matrix M_R and the diattenuation matrix M_D, from which the depolarization coefficient, retardation and diattenuation are attained respectively. Here the depolarization coefficient (Δ) is used. And through the depolarization matrix, the linear and circular depolarization coefficients (Δ_L and Δ_R) are derived which represent the depolarizing degree for linear and circular polarized light respectively. To be noted, a parameter (Δ_{LR}) reflecting the difference between linear and circular polarization is also derived. Values of Δ_{LR} larger than one mean larger linear depolarization than circular one, while the reverse for values of Δ_{LR} less than one. The brief formulae are listed below.

$$M = M_\Delta M_R M_D \tag{1}$$

$$\Delta = 1 - \frac{|trace(m_\Delta)|}{3}, 0 < \Delta < 1 \tag{2}$$

$$\Delta_L = 1 - \frac{abs\left(M_\Delta(2,2)+(M_\Delta(3,3)\right)}{2} \tag{3}$$

$$\Delta_R = 1 - abs\left(M_\Delta(4,4)\right) \tag{4}$$

$$\Delta_{LR} = \text{abs}\left(\frac{2*M(4,4)}{(M(2,2)+M(3,3))}\right) \tag{5}$$

3. Results and Discussions.

First in order to get a relatively systematic knowledge and understanding of the refractive index

matching effects on the polarization characteristics of systems of different scattering properties, we conduct Monte Carlo simulations to study the polarization features during the refractive index matching process.

Since the polarization properties of a scattering system are connected closely to the properties of the scatterers, including their sizes, densities, shapes and so on. For the sizes, the scatterers are mainly divided into two groups considering the relative ratios of their sizes with the wavelength of the incident light, including Rayleigh-scattering and Mie-scattering spherical particles. And as for the shapes of the scatterers, they may be grouped into two categories, isotropic and anisotropic shaped, typical examples are spherical and infinite-long cylindrical scatterers. Firstly the pure systems of Rayleigh-like spherical scatterers, Mie-like spherical scatterers and infinite-long scatterers are applied for investigating variation of the polarization properties with the refractive index matching and the influences of the sizes and shapes of scatterers. The results are shown in Fig.2~Fig.4.

For the pure systems of Rayleigh-scattering spherical particles, the results are shown in Fig.2, all the three depolarization coefficients (Δ, Δ_L ,Δ_R) fall with the increasing of the refractive index of the interstitial medium reflecting the reduced scattering due to RIM, and the linear depolarization coefficients are lower than those of circular ones all through the refractive index matching process indicating the scattering properties of Rayleigh-scattering particles, and which is also reflected in parameter Δ_{LR} with values less than one. As the clearing process proceeds, Δ_{LR} increases and approaches one indicating the difference of linear and circular depolarization decreases.

To study the influence of the size of the scatterers, pure systems of Mie-scattering spherical particles are considered. The results are shown in Fig. 3. The total and the linear depolarization coefficients keep the same trends as those for pure Rayleigh-scattering spherical systems mentioned above. But the circular depolarization coefficient goes up to nearly one, which means approaching total depolarization, in the beginning period of clearing, and then falls in the latter period. This phenomenon is closely related to the distribution of state of polarization of backscattered light when circular polarization is incident. And comparing the linear and circular depolarization properties, the linear depolarization is larger initially without clearing, reflecting the properties of Mie-scattering spherical particles, but as the clearing proceeds, the circular depolarization gets larger than the linear one, which means the scattering properties of the systems transform to that of Rayleigh-scattering as the discrepancy of the refractive index of the particles and medium narrows to some degree.

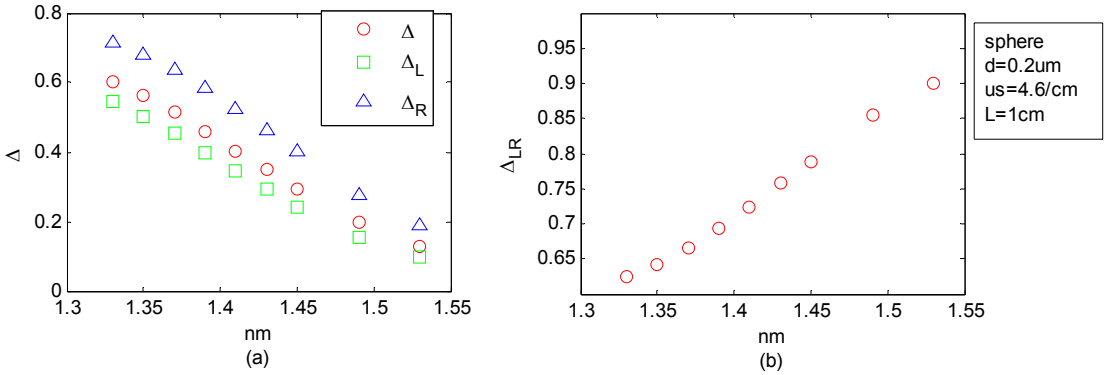

Fig. 2, Pure models of Rayleigh-scattering spherical particles. (a) The total, linear and circular depolarization coefficient marked by Δ, Δ_L and Δ_R in turn. (b) Parameter Δ_{LR} (=|2*M(4,4)/(M(2,2)+M(3,3))|). The diameter of the particle d=0.2um, the scattering coefficient without clearing us=4.6/cm. The thickness of the model L=1cm.

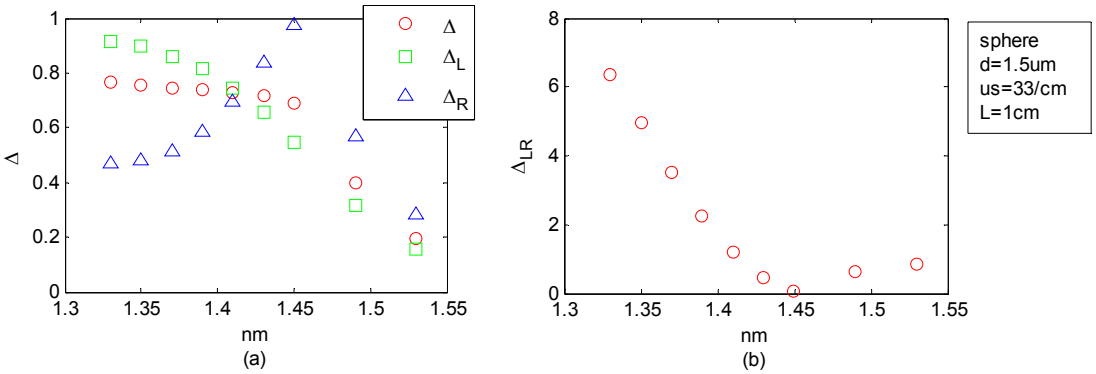

Fig. 3, Pure models of Mie-scattering spherical particles. (a) The total, linear and circular depolarization coefficient marked by Δ, Δ_L and Δ_R in turn. (b) Parameter Δ_{LR} (=|2*M(4,4)/(M(2,2)+M(3,3))|). The diameter of the particle d=1.5um, the scattering coefficient without clearing us=33/cm. The thickness of the model L=1cm.

Then the pure systems of infinite cylindrical-scattering particles are investigated. Pure systems of large scatterers are considered. Results of pure systems of small-size cylindrical scatterers are not presented, which are similar to those of systems of pure Rayleigh-like spherical scatterers. From Fig.4, linear depolarization coefficient changes slowly at first and then decreases fast and approach zero as the refractive index matching process proceeds. Circular depolarization coefficient improves to nearly one and then reduces until nearly zero during the clearing process, which is similar to the results for pure systems of Mie-like spherical particles, as shown in Fig. 3(a). To be noted, for the large-sized cylindrical scatterers, the circular depolarization coefficient is larger than the linear one, and parameter Δ_{LR} is less than one, which are different from the polarization properties of large-size

spherical scatterers but similar to those of Rayleigh-like spherical scatterers.

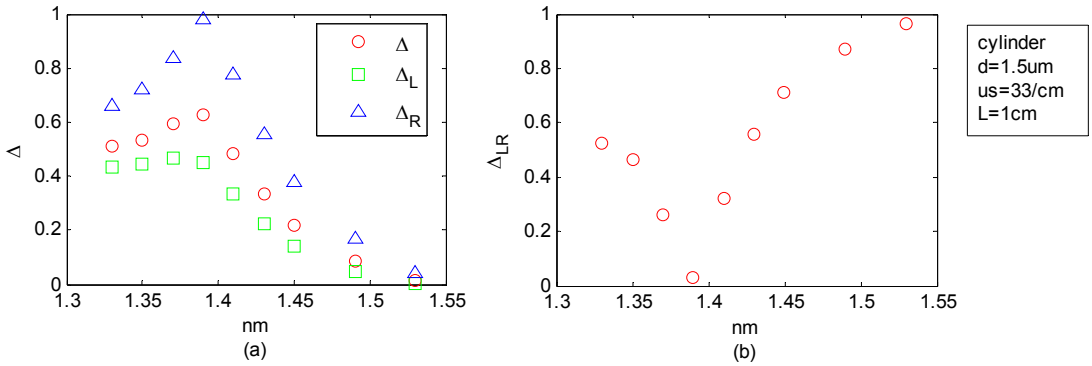

Fig. 4, Pure models of large-sized infinite-long cylindrical particles. (a) The total, linear and circular depolarization coefficient marked by Δ, Δ_L and Δ_R in turn. (b) Parameter Δ_{LR} (=|2*M(4,4)/(M(2,2)+M(3,3))|). The diameter of the particle d=1.5um, the scattering coefficient without clearing us=33/cm. The thickness of the model L=1cm.

From the above results, it is observed that, the polarization properties of pure systems of different kinds of scattering particles are different, and the circular depolarization coefficient Δ_R and parameter Δ_{LR}, can be used to differentiate pure systems of Rayleigh-like and Mie-like scattering spherical particles, and Mie-like spherical and infinite-long cylindrical scatterers during the process of refractive index matching.

Then, the hybrid systems consisted of two kinds of particles of different scattering properties are considered, including those with Rayleigh-like and Mie-like scatterers and those with Mie-like spherical scatterers and infinite-long cylindrical scatterers. For each kinds of system, different ratios of the scattering coeffients of the two components are applied. And the circular depolarization coefficient Δ_R and parameter Δ_{LR} are used to characterize the polarization properties of the samples during the clearing process.

For hybrid systems consisted of Rayleigh-like and Mie-like scatterers, the results are shown in Fig.5. It is observed that for different ratios of the scatterers, the Rayleigh-like scatterer play the main role so that parameter Δ_{LR} is smaller than one. As the ratios of Mie-like scatterers increase, the polarization properties gradually approach those of Mie-like scatterers, observing that of very high ratios of Mie-like spherical scatterers with S1/S2=1/19, with index matching increasing the circular depolarization coefficients increase first to nearly one and then decrease, and parameter Δ_{LR} decreases first and then increases, similar to the case of pure systems of Mie-like spherical scatterers, as shown in Fig.3(a).

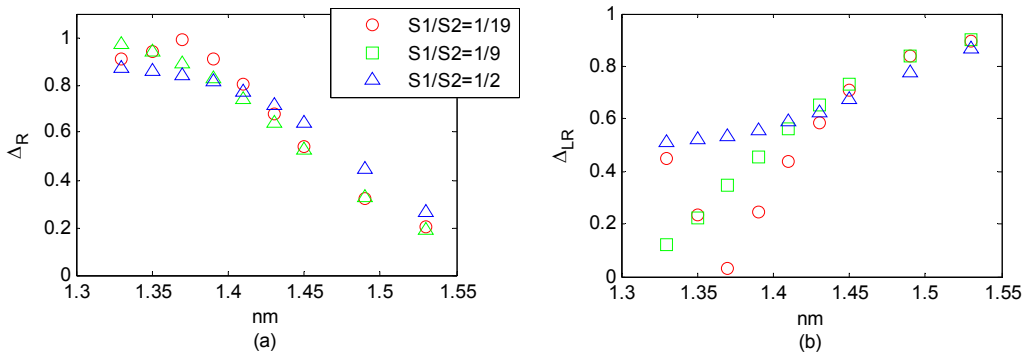

Fig. 5, Models of hybrid Rayleigh-like (S1) and Mie-like scatterers (S2). (a) The circular depolarization coefficients Δ_R for different ratios of the scatterers. (b) Parameter Δ_{LR} (=|2*M(4,4)/(M(2,2)+M(3,3))|). The total scattering coefficients are 30/cm without index matching. The diameters of scatterers are 0.2um and 1.5um respectively. The ratios (S1/S2) are 1/19, 1/9 and 1/2 in turn. The thickness of the model L=1cm.

For systems consisted of spherical scatterers and infinite-long cylindrical scatterers, the results are shown in Fig.6. Due to the diameters of both of the scatterers (=1.5um) are much larger than the wavelength of incident light (=633nm), the circular depolarization coefficients for different ratios of the scatterers first increase to nearly one and then decrease during the refractive index matching process. For different ratios of spherical and infinite-long cylindrical scatterers S/C, as the clearing process proceeds, the values of parameters Δ_{LR} decrease from more than one to nearly zero, and then increase to less than one, and this indicates that the clearing process changes the polarization properties of the systems from Mie-like scattering to Rayleigh-scattering, and this is similar to the case of pure Mie-like spherical scattering systems(as shown in Fig.3) which reflects that the polarization effects of Mie-like spherical scatterers are stronger than those of infinite-long cylindrical scatterers of the same size. From Fig. 6(b), when the degree of index matching is low, Δ_{LR} increases with the ratio of S/C, while when the degree of index matching is high enough, Δ_{LR} decreases with the ratio of S/C, so Δ_{LR} may be used to indicate the components and their ratios of sphere-cylinder systems.

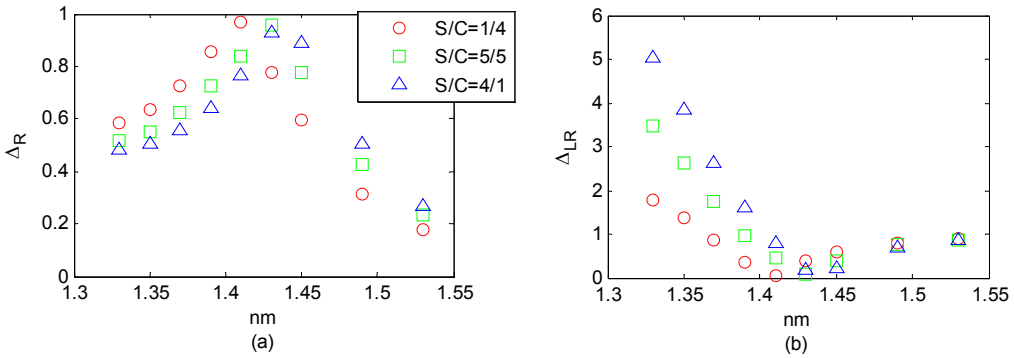

Fig. 6, Models of spherical (S) and infinite-long cylindrical scatterers (C). (a) The circular depolarization coefficients Δ_R for different ratios of the scatterers. (b) Parameter Δ_{LR} (=|2*M(4,4)/(M(2,2)+M(3,3))|). The total scattering coefficients are 30/cm without clearing. The diameters of scatterers are both 1.5um. The ratios (S/C) are 1/4, 5/5 and 4/1 respectively. The thickness of the model L=1cm.

4. Conclusion

In the context, we study the polarization features of systems of different scattering properties during the index matching process in backward detection configuration by Monte Carlo simulation. The sizes, shapes and distribution of the scatterers are varied. The linear and circular depolarization coefficients (Δ_L and Δ_R) and parameter Δ_{LR} reflecting the difference of linear and circular depolarization are used to characterize the index matching process. The results indicate that for different scattering systems, the regularities of the polarization parameters with the index matching are different, which can be used to characterize the clearing process. For all the studied scattering systems, the polarization features evolve to that of Rayleigh-like scattering when the degree of index matching is high enough. Linear depolarization coefficient decreases with index matching for all the studied scatterings systems, but the changing trends or regularities of circular depolarization coefficient and parameter Δ_{LR} are influenced by the sizes and shapes of scatterers, and the two polarization parameters can be combined to differentiate Rayleigh-like and Mie-like spherical scatterers, Mie-like spherical and infinite-long cylindrical scatterers. Then using circular depolarization coefficient and parameter Δ_{LR} for characterizing the hybrid systems, it is found that for hybrid systems containing Rayleigh-like and Mie-like spherical scatterers, the Rayleigh-like scatterers dominate the polarization features during the index matching process, and for hybrid systems containing Mie-like spherical and infinite-long cylindrical scatterers, the Mie-like spherical scatterers play the main role in polarization, and parameter Δ_{LR} may be used to obtain the ratios of the scatterers. Through this study, we examine the linear and circular polarization features of different scattering systems during the process of index matching, which are potential to be used to differentiate different scatterers and characterize the process of optical clearing. At the next stage,

the corresponding experimental studies and further analysis are planned to be made to further verify and explain the results.

Acknowledgement

The work has been supported by the National Natural Science Foundation of China. Grants Nos. 11374179, 61205199, and 41475125, and the Russian Science Foundation. Grant No. 14-15-00186.

Reference

[1]. V. V. Tuchin, L. V. Wang and D. A. Zimnyakov, [Optical Polarization in Biomedical Applications], Springer-Verlag Berlin Heidelberg, 1618-7210 (2006).

[2]. Nirmalya Ghosh and I. Alex Vitkin, "Tissue polarimetry: concepts, challenges, applications, and outlooks," Journal of Biomedical Optics 16(11), 110801 (2011).

[3]. Steven L. Jacques, J. C. Ramella-Roman and Ken Lee, "Imaging skin pathology with polarized light," Journal of Biomedical Optics 7(3), 329-340 (2002).

[4]. Angelo Pierangelo, Abdelali Benali et al., "Ex-vivo characterization of human colon cancer by Mueller polarimetric imaging," Optics Express 19(2), 1582-1593 (2011).

[5]. E Du, Honghui He et al., "Mueller matrix polarimetry for differentiating characteristic features of cancerous tissues," Journal of Biomedical Optics 19(7), 076013 (2014).

[6]. Min Xu and R. R. Alfano, "Circular polarization memory of light," Physical Review E 72, 065601(R) (2005).

[7]. C. M. Macdonald, S. L. Jacques and I. V. Meglinski, "Circular polarization memory in polydisperse scattering media," Physical Review E 91, 033204 (2015).

[8]. Valery V. Tuchin, [Tissue optics: light scattering methods and instruments for medical diagnosis], 3rd edition, PM 254, SPIE Press, Bellingham, WA, 986 (2015).

[9]. Dan Zhu, Kirill V. Larin et al., "Recent progress in tissue optical clearing," Laser Photonics Rev. 7(5), 732-757 (2013).

[10]. Valery V. Tuchin, "Optical immersion as a new tool for controlling the optical properties of tissues and blood," Laser Physics, 15(8), 1109-1136 (2005).

[11] . H. Hama, H. Kurokawa et al., "Scale: a chemical approach for fluorescence imaging and reconstruction of transparent mouse brain," Nature Neurosci. 14, 1481-1488 (2011).

[12]. Jing Wang, Yang Zhang et al., "Review: Tissue optical clearing window for blood flow monitoring," IEEE JOURNAL OF SELECTED TOPICS IN QUANTUM ELECTRONICS, 20(2),92-103 (2014). [13]. A. V. Papaev,

[13]. A. V. Papaev, G. V. Simonenko et al., “Optical anisotropy of a biological tissue under condition of immersion clearing and without them,” Optics and Spectroscopy 101(1), 46-53 (2006).

[14]. C. Macdonald and I. Meglinski, “Backscattering of circular polarized light from a dispersed random medium influenced by optical clearing,” Laser Phys. Lett 8(4), 324-328 (2011).

[15]. Dongsheng Chen, Nan Zeng et al., “Study of optical clearing in polarization measurements by Monte Carlo

simulations with anisotropic tissue-mimicking models," Journal of Biomedical Optics 21(8), 081209 (2016).
[16]. Xiang Wen, Valery V Tuchin et al., "Controlling the scattering of intralipid by using optical clearing agents," Phys. Med. Biol. 54, 6917-6930 (2009).
[17]. T. Yun, N. Zeng et al., "Monte Carlo simulation of polarized photon scattering in anisotropic media," Optics Express 17(19), 16590-16602 (2009).
[18]. Y. Guo, N. Zeng, et al., "A study on forward scattering Mueller matrix decomposition in anisotropic medium," Opt. Express, 21(15), 18361-18370 (2013).
[19]. D. Bicout and C. Brosseau et al., "Depolarization of multiply scattered waves by spherical diffusers: Influence of the size parameter," Physical Review E 49(2), 1767-1770 (1994).
[20]. S. Lu and R. Chipman, "Interpretation of Mueller matrices based on polar decomposition," J. Opt. Soc. Am. A 13(5), 1106-1113 (1996).
[21]. Sanaz Alali, Manzoor Ahmad et al., "Quantitative correlation between light depolarization and transport albedo of various porcine tissues," Journal of Biomedical Optics 17(4), 045004 (2012).